

Poisson Image Denoising Based on BLS-GSM Method

Liangdong Li¹, Nikola Kasabov², Jie Yang^{1(✉)}, Lixiu Yao¹,
and Zhenghong Jia³

¹ Institution of Image Processing and Pattern Recognition,
Shanghai Jiao Tong University, 200240 Shanghai, China
{jameslee, jieyang, lxyao}@sjtu.edu.cn

² Knowledge Engineering and Discovery Research Institute,
Auckland University of Technology, 92006 Auckland, New Zealand
nkasabov@aut.ac.nz

³ School of Information Science and Engineering,
Xinjiang University, 830046 Urumqi, China
jzh@xju.edu.cn

Abstract. Poisson noise removal is of significant importance for many applications such as spectral imaging, night vision and especially in medical imaging and astronomy. Gaussian scale mixture based methods have been widely used in image denoising. In this paper, we focus on the Poisson noise and propose a new strategy based on Bayesian least squares method for its removal. We begin with a method that removes Poisson noise by reducing it to an additive Gaussian noise with a Variance Stabilizing Transformation. Then we combine the localized version of BLS-GSM method to bring out a new denoising strategy for images corrupted by Poisson noise and experimentally show that it outperforms some of the best existing methods for Poisson noise removal both numerically and visually.

Keywords: Poisson noise removal · Variance stabilizing transformation · Gaussian noise · Localized BLS-GSM method

1 Introduction

In a wide range of imaging applications, observations are collected by counting photons hitting a detector array or vehicles passing a sensor. For example, in nuclear medicine, night vision, astronomy, traffic analysis and many other applications, there is a limited amount of available light. Even in well-lit environment, photon limitations can arise when using a spectral imager which heavily depends on the wavelength of each received photon. Thus Poisson noise removal is of significant importance in these applications above. As the noise variance equals to the expected value of the true value of observed images, Poisson noise depends on the true value. In this case, the premise of Poisson noise removal is very different from the scene of additive white Gaussian noise whose variance is usually assumed by signal processing designers and thus is known during preprocessing.

Up to now, many types of denoising methods specifically designed for Poisson noise removal have been proposed. Jin et al. [1] proposed an algorithm to restore the

Poisson noise by combining the special properties of the Poisson distribution and the idea of Optimal Weights Filter [2]. This algorithm can reconstruct the image contaminated by the Poisson noise efficiently and achieve good visual effect as well. Salmon et al. [3] proposed an algorithm which combines elements of dictionary learning and sparse patch-based representations of images. This method employs both an adaptation of Principal Component Analysis (PCA) for Poisson noise and recently developed sparsity-regularized convex optimization algorithms for photon-limited images. Deledalle et al. [4] proposed an extension of the NL-means for images contaminated by the Poisson noise, based on probabilistic similarities to compare noisy patches and patches of a pre-estimated image, and on a minimization of the Mean Square Error (MSE) with respect to the denoising parameters. There are also many other methods (see [5, 6] for detail about the multiscale maximization a priori method and [7, 8] for regularization based on a total variation semi-norm).

Different from the algorithms mentioned above, the most popular methods of Poisson noise removal are usually performed by reducing it to nearly additive Gaussian noise through the following three steps. Firstly, the variance of the Poisson noise is stabilized by applying a Variance Stabilizing Transformation (VST) such as Anscombe root transformation [9], so that the transformed data are approximately homoscedastic and Gaussian. This step will produce a noisy image data in which the noise can be handled as additive Gaussian noise with unitary variance. Secondly, the noise is removed by a conventional denoising method for additive Gaussian white noise such as NL-means [10], BM3D [11] and BLS-GSM [12]. Thirdly, an inverse transformation is applied to the denoised data, obtaining the estimate of the signal of interest. Makitalo et al. [13, 14] focused on the last step, and introduce the Exact Unbiased Inverse (EUI) method. Authors [15–17] improved both the first and last step and achieved remarkable denoising results.

In this paper, we focus on a strategy for Poisson noise removal based on BLS-GSM [12, 18]. We begin with a Variance Stabilizing Transformation method that suppresses Poisson noise to an additive Gaussian noise with unitary variance. Then we combine the localized version of BLS-GSM method to bring out a new denoising strategy for images contaminated by Poisson noise. We will show that the resulting method is state-of-the-art in terms of PSNR.

The paper is organized as follows: in Sect. 2 we explain the Poisson noise removal problem with more details about VST, EUI, and BLS-GSM, and then propose our three-stage algorithm for Poisson denoising. In Sect. 3 we conduct some experiments and analysis to prove that EUI combined with localized BLS-GSM gives rise to a very efficient filtering solution that is competitive with some of the best existing methods for Poisson noise removal. In Sect. 4 we make some discussions to conclude this paper.

2 Method Description

2.1 Poisson Noise

Let $x_i, i = 1, \dots, N$ be the observed pixel values obtained through an image sensor where x_i is an independent random Poisson variable whose mean $y_i \geq 0$ is the underlying intensity value to be estimated. Thus the discrete Poisson probability of each x_i is:

$$P(x_i|y_i) = \frac{y_i^{x_i} e^{-y_i}}{x_i!}. \tag{1}$$

As the mean of the Poisson variable is equal to its variance, so we have

$$E\{x_i|y_i\} = y_i = var\{x_i|y_i\}. \tag{2}$$

As we have mentioned above, the noise variance depends on the true intensity value, thus Poisson noise is signal dependent.

2.2 Our Algorithm

In this subsection we present our algorithm for removing Poisson noise and discuss in full detail in the following.

A standard way to denoise Poisson noise image is using a variance stabilizing transformation (VST). To remove the data-dependence of the noise variance, we apply VST to make it constant throughout the whole denoising procedure with a conventional Gaussian denoising method. In the recent years, many variance stabilization transforms have been developed [15–17], among which the most popular VST is the Anscombe transformation [9]:

$$f(x) = 2\sqrt{x + \frac{3}{8}}. \tag{3}$$

However, applying (3) directly to Poisson distributed data can only produce an approximately Gaussian distributed data with variance 1. This holds still when the mean of the Poisson data is greater than 4. The denoising of $f(x)$ produces a signal \mathbf{D} that can be considered as an estimate of $E\{f(x)|y\}$. We will discuss later on.

After applying the Anscombe transformation, we need to apply conventional denoising technique for Gaussian noise such as Bayes Least Squares – Gaussian Mixture Model (BLS-GSM) method [12]. Instead of using it directly, we introduce an improved version (i.e. localized BLS-GSM). For rigorous reason we make some discussion and show more details than the original paper. The basic mind of the algorithm is to model a noiseless wavelet coefficient neighborhood \mathbf{x} , by a Gaussian scale mixture which is defined as

$$\mathbf{x} = \sqrt{m}\mathbf{u} \tag{4}$$

where \mathbf{u} is a zero-mean Gaussian random vector and m an independent positive scalar random variable. Without loss of generality, we can assume the expectation of $E\{m\} = 1$. Thus we have $\mathbf{C}_x = \mathbf{C}_u$, where \mathbf{C} represents the covariance matrix of a vector. The idea of denoising is as follows: (1) decompose the noisy input image into a wavelet pyramid, (2) apply the whole denoising process on wavelet coefficients, (3) obtain the final denoised image by reconstruction. Besides, to avoid ringing artifacts in the reconstruction, a redundant version of wavelet transform steerable pyramid is

used. For an $n_1 \times n_2$ image, the steerable pyramid is generated in $\log_2(\min(n_1, n_2)) - 4$ scales and eight orientations. Assume that the image is contaminated by independent additive Gaussian noise. Thus, a typical neighborhood of wavelet coefficients can be written as

$$\mathbf{y} = \mathbf{x} + \mathbf{w} = \sqrt{m}\mathbf{u} + \mathbf{w} \tag{5}$$

where \mathbf{y} is the observed noisy neighborhood to be estimated, \mathbf{x} the original neighborhood and \mathbf{w} the independent additive white Gaussian noise signal with known variance σ . With the observed noisy vector \mathbf{y} , a Bayes Least Square (BLS) estimation of x , $E\{x|\mathbf{y}\}$ is calculated as follows

$$E\{x|\mathbf{y}\} = \int_0^\infty p(z|\mathbf{y})E\{x|\mathbf{y}, z\}dz. \tag{6}$$

According to the original work [12], discrete form of $E\{x|\mathbf{y}\}$ can be computed as

$$E\{x|\mathbf{y}\} = \sum_{i=1}^{13} p(\log_e(z_i)|\mathbf{y})E\{x|\mathbf{y}, \log_e(z_i)\}. \tag{7}$$

To get $E\{x|\mathbf{y}\}$, we just need to calculate $p(\log_e(z_i)|\mathbf{y})$ and $E\{x|\mathbf{y}, \log_e(z_i)\}$ respectively. For notational simplicity, we replace the $\log_e(z_i)$ term with z_i . The detailed derivation process of the two components can be found in [12]. Therefore, we omit the details in this paper and thus we have:

$$E\{x|\mathbf{y}, z_i\} = z\mathbf{M}\mathbf{A}(z\mathbf{\Lambda} + \mathbf{I})^{-1}\mathbf{v} \tag{8}$$

where $\mathbf{C}_w = \mathbf{S}\mathbf{S}^T$, $\mathbf{Q}\mathbf{A}\mathbf{Q}^T = \mathbf{S}^{-1}\mathbf{C}_u(\mathbf{S}^{-1})^T$, $\mathbf{M} = \mathbf{S}\mathbf{Q}$, $\mathbf{v} = \mathbf{M}^{-1}\mathbf{y}$.

The discrete form of $p(z_i|\mathbf{y})$ is

$$p(z_i|\mathbf{y}) = \frac{p(\mathbf{y}|z_i)p_z(z_i)}{\sum_{j=1}^{13} p(\mathbf{y}|z_j)p_z(z_j)} \tag{9}$$

where $p_z(z_i) \propto \frac{1}{z_i}$.

The main point of this procedure is to use any wavelet coefficient, either extracted from a single orientation/scale or mixing orientations and scales. The idea is to denoise all these wavelet coefficients in the pyramid, and then a reconstruction step of the denoised image is performed by the inverse pyramid.

After discussing the BLS-GSM method, we realize the denoising procedure by firstly partition the input $n_1 \times n_2$ noisy image into $\sqrt{d} \times \sqrt{d}$ blocks, where $d = \min([\sqrt{n_1}], [\sqrt{n_2}])$. And then we apply BLS-GSM to each block.

Having finished the two successive steps above, the only work we need to do is applying an inverse transformation to \mathbf{D} in order to obtain the denoised estimate of \mathbf{y} . In [13] the authors proposed three inverse transformations: algebraic inverse,

asymptotically unbiased inverse and exact unbiased inverse. In this paper we just focus on the EUI method which will be discussed in the following.

Given a perfect denoising, that is to say \mathbf{D} can be treated as $E\{f(x)|y\}$, and the EUI of the Anscombe transformation f is an inverse transformation:

$$T : E\{f(x)|y\} \mapsto E\{x|y\}. \quad (10)$$

As mentioned in 2.1, for any given y , we have $E\{x|y\} = y$. Then the problem of finding the inverse transformation T reduces to computing the values $E\{f(x)|y\}$ defined as:

$$E\{f(x)|y\} = \int_{-\infty}^{+\infty} f(z)p(z|y)dz, \quad (11)$$

where $p(z|y)$ is the generalized probability density function of z conditioned on y . For discrete Poisson probabilities $P(x|y)$, we have the following form:

$$E\{f(x)|y\} = \sum_{x=0}^{+\infty} f(x)P(x|y). \quad (12)$$

Take (1) and (3) into consideration, we have the finally form:

$$E\{f(x)|y\} = 2 \sum_{x=0}^{+\infty} \left(\sqrt{x + \frac{3}{8}} \cdot \frac{y^x e^{-y}}{x!} \right). \quad (13)$$

To solve the problem of approximately transformation mentioned at the beginning of 2.2, for data in \mathbf{D} that is greater than $2\sqrt{3/8}$, we set to 0.

3 Experiments and Analysis

Having introduced the main strategy in Sect. 2, in this section we implement our algorithm and make comparison with other Poisson denoising methods. As described above we will perform our method in three successive steps: (1) an Anscombe VST is used to stabilize the Poisson noise variance. (2) the localised BLS-GSM method is used for denoising the signal produced in the last step, which can be treated as additive white Gaussian noise. (3) the exact unbiased inverse is applied to the denoised signal, obtaining the estimate of the signal of interest. In the second step, we compare the performance of the localized BLS-GSM method with a few recent classic denoising algorithms for Gaussian noise removal: NL-means [10], K-SVD [19], BM3D [11]. We also conduct comparisons against algorithms specifically designed for Poisson noise removal such as Weights Optimization Filter (WOF) [1], Non-local PCA [3] and Unsupervised Non-local Means (UNL-Means) [4].

To describe quantitatively performance of denoising results, two classic measures are introduced, the Root Mean Square Error (RMSE) and Peak Signal to Noise Ratio (PSNR). The RMSE is computed as:

$$RMSE = \sqrt{\frac{\sum_i (\hat{y}_i - y_i)^2}{N}},$$

where \hat{y}_i represents the estimated intensities, y_i the respective true value, N the total number of pixels in the image. The smaller the RMSE, the better the denoising. The PSNR is evaluated in decibels (dB):

$$PSNR = 20\log_{10}\left(\frac{\max(y_i)}{RMSE}\right).$$

The larger the PSNR, the better the denoising.

To make objective and balanced comparisons, we conduct our experiments with the set of test images all of which are 256×256 in size provided by the authors of [17] showing in Fig. 1. They are Spots [0.03, 5.02], Galaxy [0, 5], Ridges [0.05, 0.85], Barbara [0.93, 15.73] and Cells [0.53, 16.93]. These test images can be downloaded from <http://www.cs.tut.fi/foi/invansc/>. Table 1 provides the numerical denoising results of these noise removal methods in terms of PSNR(dB)/RMSE. The experiments results show that the Localized BLS-GSM method is competitive with the more recent denoising algorithms specifically designed for Poisson noise removal [1, 3] which achieve excellent denoising results. Figures 2 and 3 show the visual quality performance of these methods and the comparison of our strategy with other noise removal methods.

As shown in the Figs. 2 and 3, the Localized BLS-GSM algorithm preserves the sharpness of edges. The denoised images preserve more detail of the original ones than NL-Means(e), K-SVD(f) and UNL-Means(i) although a little inferior to BM3D ones. Besides, it also introduces fewer artifacts than most of the other methods. Overall, the visual performance is superior to most of the other recently proposed Poisson noise removal algorithms, while a little inferior to the BM3D's.

All in all, the performance of the Localized BLS-GSM algorithm is state-of-the-art in terms of both visual quality and numerical results of PSNR/RMSE.

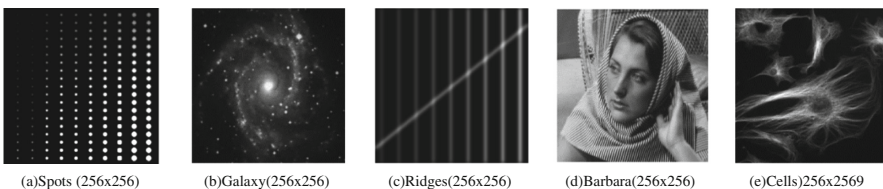


Fig. 1. Original test images used in the experiments.

Table 1. The numerical comparison in terms of PSNR/RMSE between LBS-GSM combined with VST for Poisson noise removal method and other algorithms including Conventional Gaussian denoising methods and specifically designed for Poisson noise removal. The intensity range of each image is indicated in brackets.

	Conventional Gaussian denoising methods combined with VST					Specifically designed for Poisson noise removal methods		
	LBS-GSM	BM3D [11]	NL-Means [10]	K-SVD [19]	WOF [1]	NL-PCA [3]	UNL-Means [4]	
Spots [0.03,5.02]	31.47/0.1472	31.96/0.1267	29.98/0.2237	30.25/0.1672	31.52/0.1410	31.08/0.1522	30.58/0.1568	
Galaxy [0.5]	29.37/0.1485	28.05/0.1980	26.69/0.3321	27.11/0.2120	29.37/0.1485	28.62/0.1913	27.24/0.2098	
Ridges [0.05,0.85]	24.01/0.0568	24.54/0.0507	22.68/0.1030	23.87/0.0763	24.13/0.0520	24.54/0.0507	23.67/0.0800	
Barbara [0.93,15.73]	26.44/0.6493	25.92/0.7956	24.97/0.9602	25.11/0.8972	25.78/0.8239	26.03/0.6233	25.32/0.8879	
Cells [0.53,16.93]	30.67/0.4936	30.19/0.5240	28.71/0.8783	29.33/0.5567	29.62/0.5015	30.10/0.5103	28.99/0.8023	

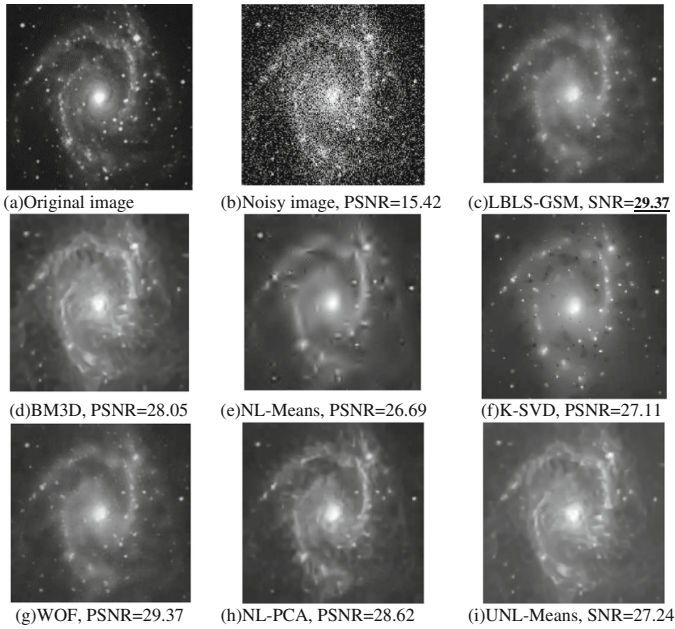


Fig. 2. Visual quality comparison between LBLS-GSM algorithms and others of Galaxy.



Fig. 3. Visual quality comparison between LBLS-GSM algorithms and others of Galaxy.

4 Discussion and Conclusion

In this part we present the experiments results and make some conclusions.

A new strategy for denoising images corrupted by Poisson noise is implemented. By combining the Localized BLS-GSM method with VST we implement Poisson noise removal effectively. Compared with other conventional Gaussian noise removal method and algorithms specifically designed for Poisson noise removal, the LBLGS-GSM can achieve excellent effect in terms of both visual quality and numerical results of PSNR/RMSE.

Acknowledgement. This research is partly supported by NSFC, China (No: 61273258) and 863 Plan, China (No. 2015AA042308).

References

1. Jin, Q., Grama, I., Liu, Q.: A new poisson noise filter based on weights optimization. *J. Sci. Comput.* **58**(3), 548–573 (2014)
2. Jin, Q., Grama, I., Liu, Q.: Removing gaussian noise by optimization of weights in non-local means. *arXiv*, preprint [arXiv:1109.5640](https://arxiv.org/abs/1109.5640) (2011)
3. Salmon, J., et al.: Poisson noise reduction with non-local PCA. *J. Math. Imaging Vis.* **48**(2), 279–294 (2014)
4. Deledalle, C.-A., Tupin, F., Denis, L.: Poisson NL means: unsupervised non local means for poisson noise. In: 17th IEEE International Conference on Image Processing (ICIP), pp. 801–804. IEEE (2010)
5. Nowak, R., Kolaczyk, E.D.: A multiscale MAP estimation method for poisson inverse problems. In: *Signals, Systems & Computers, Conference Record of the Thirty-Second Asilomar Conference on*, vol. 2, pp. 1682–1686. IEEE (1998)
6. Nowak, R.D., Kolaczyk, E.D.: A statistical multiscale framework for Poisson inverse problems. *IEEE Trans. Inf. Theory* **46**(5), 1811–1825 (2000)
7. Bardsley, J.M., Luttman, A.: Total variation-penalized Poisson likelihood estimation for ill-posed problems. *Adv. Comput. Math.* **31**(1-3), 35–59 (2009)
8. Beck, A., Teboulle, M.: Fast gradient-based algorithms for constrained total variation image denoising and deblurring problems. *IEEE Trans. Image Process.* **18**(11), 2419–2434 (2009)
9. Anscombe, F.J.: The transformation of poisson, binomial and negative-binomial data. *Biometrika* **35**, 246–254 (1948)
10. Buades, Antoni, Coll, Bartomeu, Morel, Jean-Michel: A review of image denoising algorithms, with a new one. *Multiscale Model. Simul.* **4**(2), 490–530 (2005)
11. Dabov, K., Foi, A., Katkovnik, V., Egiazarian, K.: Image denoising by sparse 3D transform-domain collaborative filtering. *IEEE Trans. Image Process.* **16**(8), 2080–2095 (2007)
12. Portilla, J., Strela, V., Wainwright, M.J., Simoncelli, E.P.: Image denoising using scale mixtures of Gaussians in the wavelet domain. *IEEE Trans. Image Process.* **12**, 1338–1351 (2003)
13. Makitalo, M., Foi, A.: On the inversion of the Anscombe transformation in low-count Poisson image denoising. In: *International Workshop on Local and Non-Local Approximation in Image Processing, LNLA 2009*. IEEE (2009)

14. Makitalo, M., Foi, A.: Optimal inversion of the Anscombe transformation in low-count Poisson image denoising. *IEEE Trans. Image Process.* **20**(1), 99–109 (2011)
15. Lefkimmiatis, S., Maragos, P., Papandreou, G.: Bayesian inference on multiscale models for Poisson intensity estimation: applications to photon-limited image denoising. *IEEE Trans. Image Process.* **18**(8), 1724–1741 (2009)
16. Luisier, F., et al.: Fast interscale wavelet denoising of poisson-corrupted images. *Signal Process.* **90**(2), 415–427 (2010)
17. Zhang, B., Fadili, J.M., Starck, J.L.: Wavelets, ridgelets, and curvelets for Poisson noise removal. *IEEE Trans. Image Process.* **17**(7), 1093–1108 (2008)
18. Rajaei, B.: An analysis and improvement of the BLS-GSM denoising method. *Image Process. Line* 44–70 (2014)
19. Lebrun, M., Leclaire, A.: An mplementation and detailed analysis of the K-SVD image denoising algorithm. In: *Image Processing on Line* (2012)